Journal of the European Ceramic Society 19 (1999) 1187–1190

PII: S0955-2219(98)00401-4
0955-2219/99/$ - see front matter

# Effect of Nb, Li Doping on Structure and Piezoelectric Properties of PZT Type Ceramics

C. Tănăsoiu, E. Dimitriu* and C. Miclea

National Institute for Materials Physics, 96700 Măgurele-Bucharest, PO Box MG-7, Romania


## Abstract

*The effect of niobium and lithium doping on the structure and piezoelectric properties of some samples with the following compositions* $PbZr_{0\cdot051}Nb_3Li)_xTi_{0\cdot49\text{-}x}O_3$*, with* $0{\cdot}015 \leq x \leq 0{\cdot}050$*, was investigated. The materials were prepared by the usual ceramic technique using high purity raw materials. Disc shaped samples of each composition were sintered at temperatures between 1200 and 1300°C, for 4 h. The samples structure was determined by X-ray diffractometry and the piezoelectric properties were determined by means of resonance–antiresonance method, using a HP 4194A impedance gain phase analyser. A morphotropic phase boundary (MPB) with the optimum piezoelectric properties was found around the compositions with* $x = 0{\cdot}020$*. The optimum values for relative dielectric constant* $\varepsilon_r$*, planar electromechanical coupling factor* $k_p$*, and mechanical quality factor* $Q_m$ *of about 1700, 0·59 and 75, respectively, were found for these compositions. The lattice constants* a *and* c *of rhombohedral and tetragonal phases were determined by means of an X-ray* CuKα *diffractometer. The results are discussed in terms of the domain easy switching phenomena and high poling degree, brought about by the A-vacancies produced by the NbLi pairs doping. © 1999 Elsevier Science Limited. All rights reserved*


*Keywords*: morphotropic phase boundary, piezoelectric properties, PZT.

## 1 Introduction

Piezoelectric ceramics of $Pb(ZrTi)O_3$ type solid solutions have achieved wide usage in recent years because of their superior properties.[1] The application of the piezoelectric materials is almost unlimited and it depends only on the skill of the users. It is sufficient to mention the newest and most exciting applications of such ceramics for piezoelectric micromotors,[2–6] microrobots,[7] actuators,[8,9] the moonie composite transducers,[10] control of displacement and positioning systems,[11–15] to understand the importance of piezoelectric materials with improved characteristics. Therefore any efforts directed towards searching for new piezoelectric ceramic materials are worthwhile.

The present investigation was devoted to the study of the effect of doping with $(Nb_3Li)$ pair on the main properties of soft type PZT materials. The doped material was $Pb(Zr_{0\cdot51}Ti_{0\cdot49})O_3$ i.e. a usual PZT composition situated close to the morphotropic phase boundary (MPB), according to the phase diagram of the $PbTiO_3$–$PbZrO_3$ solid solution.[1] For the compositions situated near the MPB both tetragonal (Ti rich) and rhombohedral (Zr rich) structures can be present.

Higher valence substituents like $Nb^{5+}$ contribute electrons, being thus a donor, enter the B site into the lattice and may create A vacancies,[1] while lower valence ones like $Li^+$, acting as an acceptor, could also enter the A site and create some A type vacancies, but with a slight effect on material characteristics.

Therefore we tried a dopant combination of Nb and Li, with more Nb and less Li, in such a manner that the valency to be compensated and we found that three $Nb^{5+}$ and one $Li^+$ gave the equivalent of four +4 valency ions.

## 2 Experimental

The general chemical formula for the investigated compositions is as follows:

$Pb[Zr_{0\cdot51}Ti_{0\cdot45\text{-}x}(Nb_3Li)_x]O_3$. There have been prepared six compositions with $x = 0{\cdot}005$, 0·010, 0·020, 0·030, 0·040 and 0·050.

The method used was the usual ceramic technique involving the following main steps: weighing the stoichiometric quantities of raw oxides; mixing the oxidic materials of 99·9% purity in a planetary mill, in agate vessels, in methanol, for 2 h, calcining the dried mixture at 880°C for 4 h, in dense alumina crucible; milling the calcined product for 6 h;

*To whom correspondence should be addressed. E-mail: edimit@alpha1.infim.ro

pressing the milled powder as discs with 10 mm diameter and 1 mm thick; sintering the samples at temperatures between 1200 and 1300°C for 4 h; mechanically processing the sintered samples and silver electrodes; poling the samples in a silicon oil bath at 200°C under a 3 kV mm$^{-1}$ electric field, measuring the piezoelectric parameters, 24 h after poling, by means of a HP 4194A impedance/gain phase analyser.

## 3 Results

The main results are shown in Figs 1–4. Figure 1 shows the behaviour of the relative dielectric constant $\varepsilon_r$ as a function of dopants concentration for the three different sintering temperatures. The maximum values of $\varepsilon_r$ obtained for each sintering temperature are centred around the composition with $x = 0{\cdot}020$.

Figure 2 shows the behaviour of electromechanical coupling coefficient $k_p$ as a function of dopant level for different sintering temperatures. Here also, the maximum values of $k_p$ correspond to composition with $x = 0{\cdot}020$.

Figure 3 shows the dependence of the mechanical quality factor on composition. One observes that $Q_m$ shows minimum values (under 100) for the same composition with $x = 0{\cdot}020$. The low values of $Q_m$ are characteristic for soft type ferroelectric materials.

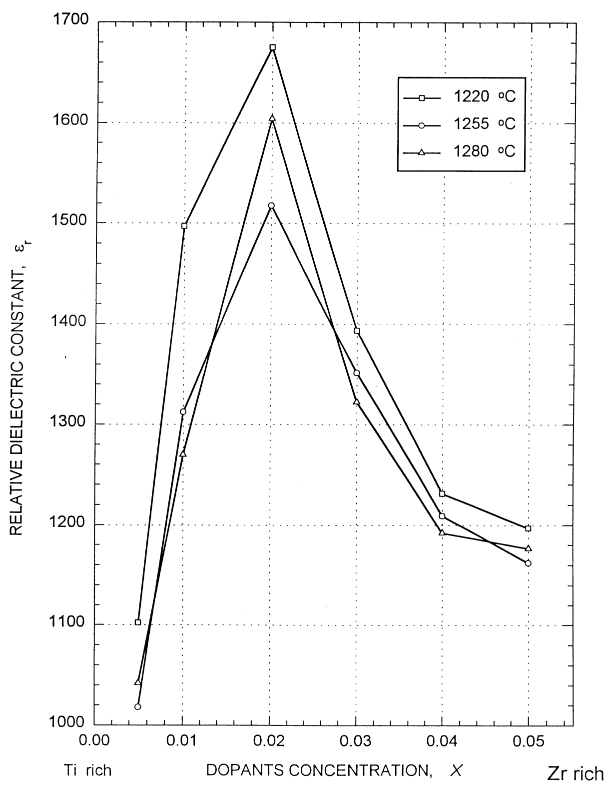


**Fig. 1.** The behaviour of relative dielectric constant $\varepsilon_r$, as a function of dopants concentration, for three different sintering temperatures.

Figure 4 presents the dependence of piezoelectric charge constants $d_{33}$ on composition. Again high values are observed for samples with $x = 0{\cdot}020$.

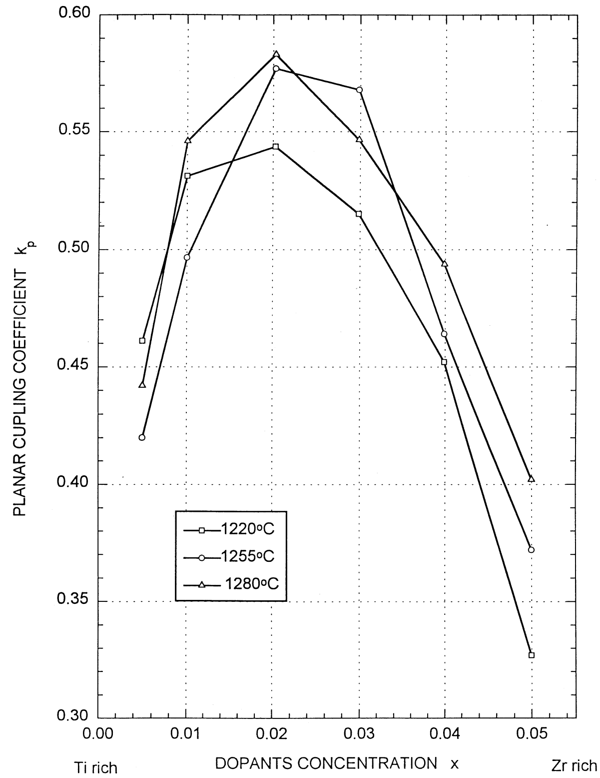


**Fig. 2.** The behaviour of the electromechanical planar coupling coefficient $k_p$ as a function of dopant concentration, for samples sintered at three different temperatures.

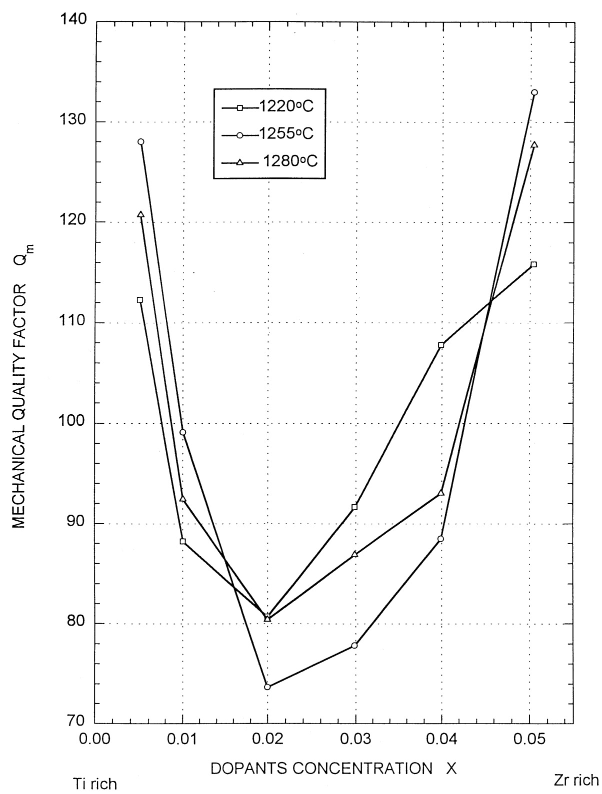


**Fig. 3.** Mechanical quality factor $Q_m$ for samples sintered at three different temperatures.

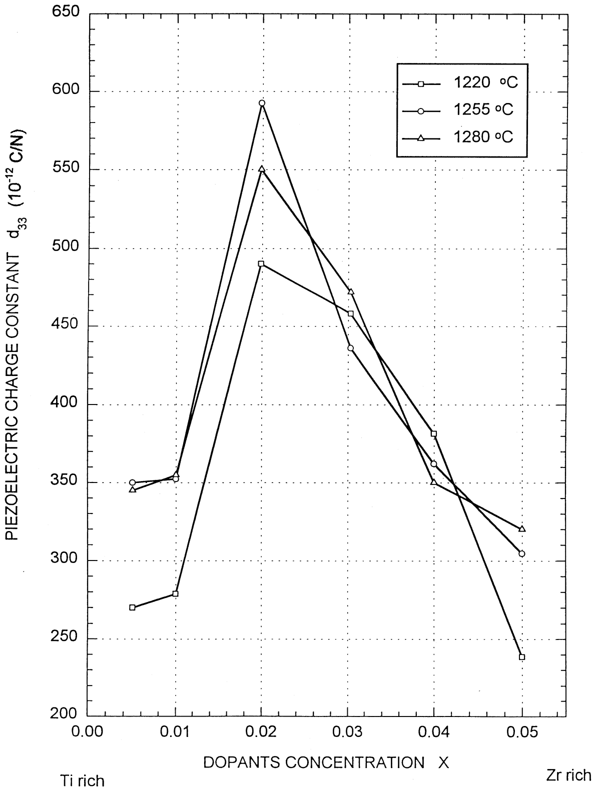


**Fig. 4.** Piezoelectric charge constant $d_{33}$ as a function of dopants concentration, for three different sintering temperatures

**Table 1.** Lattice parameters $a_T$, $c_T$ for T phase and $a_R$, $c_R$ for R phase for $Nb_3Li$ doped composition. (One may notice the existence of both T and R phase for composition with $x = 0{\cdot}020$.)

| x | *T phase* | | *R phase* | |
|---|---|---|---|---|
| | $a_T$(Å) | $c_T$(Å) | $a_R$(Å)[a] | $c_R$(Å)[a] |
| 0·005 | 4·037 | 4·131 | — | — |
| 0·010 | 4·042 | 4·093 | — | — |
| 0·020 | 4·063 | 4·111 | 4·316 | 9·001 |
| 0·030 | — | — | 5·788 | 7·094 |
| 0·040 | — | — | 5·792 | 7·702 |
| 0·050 | — | — | 5·818 | 7·056 |

[a]Hexagonal axes were used for rhombohedral lattice.

It is obvious from these figures that all piezoelectric properties show optimum values, with a rather sharp maximum, for compositions situated around $x = 0{\cdot}020$. This is a clear indication that these compositions must be situated within a morphotropic phase zone where tetragonal and rhombohedral structures may coexist.

The chemical formula for these ceramics correspond to: $Pb[Zr_{0{\cdot}51}Ti_{0{\cdot}47}\,(Nb_{0{\cdot}015}Li_{0{\cdot}05})]O_3$, characteristics for soft type piezoceramics.

## 4 Discussion

The behaviour of the piezoelectric properties as a function of the composition shown in Figs 1–4 can be qualitatively explained in terms of the possible structures of the doped composition. Thus, the left side composition, namely the low doped ones, are Ti richer and normally tetragonally distorted (T phase) according to the current version of the PZT phase diagram (see for instance Ref. 1 pp. 135–136). The right side ones (highly doped) containing a higher Zr:Ti content should be rhombohedrally distorted (R phase). The piezoelectric parameters for all these end compositions show lower values. The compositions situated within these phases must be both T and R distorted, the effect being more pronounced for compositions situated at the middle of the diagram.

The X-ray difractograms (not shown here) made in the region including (200)T and (002)T reflection as well as (200)R reflection, for $2\theta$ ranging between 43° and 46°, showed clearly the existence of T phase for low doped samples and R phase for higher doped ones and the presence of both phases for those corresponding to $x = 0{\cdot}002$.

The composition with $x = 0{\cdot}002$ contains both T and R phases in equal quantities and favours strong piezoelectric effect due to the increased ease of reorientation during poling by transformation of a number of 180° domains into 90° ones. Therefore it appears that the MPB zone of the solid solutions investigated is situated around composition with $x = 0{\cdot}002$.

## 5 Conclusion

A usual PZT type material was doped with $Nb_3Li$ pairs in the range 0·5–5% at. and compositions with maximum piezoelectric characteristics were found for a doping level of 2%. These compositions are believed to be situated in a MPB zone where the ferroelectric domains can be easier aligned along the electric field during poling thus making possible a higher poling degree and higher piezoelectric characteristics.

## References

1. Jaffe, B., Cook, W. R. and Jaffe, H., *Piezoelectric Ceramics*. Academic Press, London, New York, 1971, pp. 271–281.
2. Wallaschek, J., Piezoelectric ultrasonic motors. *J. Intell. Mat. Syst. Structures*, 1995, **6**, 71–73.
3. Yamayoshi, Y. and Hirose, H., Ultrasonic motors not using mechanical friction force. *Int. J. Appl. Electr. Mat*, 1992, **3**, 179–182.
4. Tomikawa, Y. and Ogasawa, T., Ultrasonic motors: construction, characteristics, applications. *Ferroelectrics,*, 1989, **91**, 13–178.
5. Tomikawa, Y., Ogasawa, T., Suyawara, S., Konno, M. and Takano, T., Construction of ultrasonic motors and their applications. *Jap. J. Appl. Phys*, 1988, **27**, 195–197.
6. Kumada, A., A piezoelectric ultrasonic motor. *Jap. J. Appl. Phys*, 1985, **24**, 739–741.
7. Smith, L.G., Design considerations of a piezoelectric on-silicon microrobot. *Sensors and Actuators*, 1992, **A35**, 129–135.

8. Flint, E., Liang, C. and Rogers, C. A., Electromechanical analysis of piezoelectric stack active member power consumption. *J. Intell. Mat. Syst. Structures*, 1995, **6**, 117–124.
9. Sun, F. P., Chandhry, Z., Liang, C. and Rogers, C. A., Truss structure integrity identification using PZT sensor actuator. *J. Intell. Mat. Syst. Structures*, 1995, **6**, 134–139.
10. Onitsuka, K., Dogan, A., Tressler, J. F., Xu, Q, Yoshikawa, S. and Newnham, R. E., Metalic ceramic composite transducer, the Moonie. *J. Intell. Mat. Syst. Structures*, 1995, **6**, 447–455.
11. Robbins, W. P., Polla, D. L., Tamagawa, T., Glumac, D. E. and Tyhen, W., Design of linear motion microactuator using piezoelectric thin films. *J. Micromech. Microeng*, 1991, **1**, 247–252.
12. Overshuzen, T. and Watson, G., URV piezoelectric translator. *Nucl. Instr*, 1986, **A246**, 787–789..
13. Renner., C., Niedermann, P., Kent, A. O. and Fisher, O, A vertical piezoelectric inertial slider. *Rev. Sci. Instrum.*, 1990, **61**, 965–967.
14. Duong, K. and Garcia, E., Open loop compensation in a stack-mass positioning system. *J. Intell. Mat. Syst. Structures*, 1995, **6**, 292–296.
15. Matsko, M. G., Xu, Q. and Newnham, R. E., Zig-zag piezoelectric actuators: geometrical control of displacement and resonance. *J. Intell. Mat. Syst. Structures*, 1995, **6**, 783–786.